0254-6124/2005/25(5)-484-06 *Chin. J. Space Sci.* 空间科学学报

Gao H, Xi J Y, Yuan W. A method of inversing the peak density of atomic oxygen distribution in the MLT region from the ground-based OI (557.7 nm) night airglow observation. *Chin. J. Space Sci.*, 2005, **25**(5): 484—489

A Method of Inversing the Peak Density of Atomic Oxygen Vertical Distribution in the MLT Region From the OI (557.7 nm) Night Airglow Intensity*

H. Gao[1,2,3] J. Y. Xu[1,2] W. Yuan[1,2]

[1](*Laboratory for Space Weather, Center for Space Science and Applied Research, Chinese Academy of Sciences, Beijing* 100080, *China*)

[2](*China-Russia Joint Research Center on Space Weather*)

[3](*Graduate School, Chinese Academy of Sciences, Beijing* 100039)

Abstract In this paper, using the MSISE-90 model as the reference atmosphere, we discuss the feasibility and method of deducing the peak densities of the undisturbed atomic oxygen profiles in the MLT region (the mesosphere and lower thermosphere region) from OI (557.7 nm) night airglow intersities. The peak densities for different seasons, latitudes and longitudes are deduced from OI (557.7 nm) airglow intensities through this expression. We analyze the features of inversion relative errors and discuss the influence of the variations in temperature on inversion errors. The results indicate that all inversion errors are less than 5% except for those at high altitudes in the summer hemisphere. And the impact of the variations in temperature on errors is not significant.

Key words OI (557.7 nm) airglow intensity, Mesopause, Atomic oxygen distribution, Peak density

1 Introduction

The MLT region is an important region where the coupling between the middle and the upper atmosphere and the transition from well-mixed eddy mixing gas to molecular diffusion equilibrium gas occur. In this region, the chemical lifetime of atomic oxygen is longer than one day and the vertical gradient of atomic oxygen is large, so the vertical distribution of atomic oxygen is controlled by the photochemical processes and affected by the dynamical processes[1]. At the same time, atomic oxygen affects many photochemical processes and energy budget in the MLT region. Therefore, atomic oxygen is one of the fundamental research topics in aeronomy.

Because of the inaccessibility of the MLT region to both balloons and satellites and the intrinsic sporadic nature of in situ rocket experiments, remote sensing of airglow is a viable way to measure atomic oxygen distribution in the MLT region. There are two approaches to obtain atomic oxygen density profiles by remote sensing of airglow. One is realized through exploring the vertical distribution of oxygen airglow volume emission rate, such as measurement of molecular oxygen nightglow emission[2],[3], measurement of OH glow emission[2],[4]–[6], measurement of OI (557.7 nm) line volume emission rate profile[3],[7]–[10], and so on. However, it is difficult to determine the time variation of atomic oxygen density through this approach. The other one is realized through measuring the ground-based integrated night airglow intensities. It is based on the Chapman distribution of the atomic oxygen profile[11]–[14]: $[\mathrm{O}]_z = [\mathrm{O}]_\mathrm{m} \exp \frac{1}{2}\left[1 - \frac{z - z_\mathrm{m}}{S \cdot H} - \exp \frac{-(z - z_\mathrm{m})}{S \cdot H}\right]$, the expressions for pertinent airglow volume emission rates. The three parameters in the Chapman distribution can be inversed either by the OI (557.7 nm) night airglow intensity and OH glow emission intensity or by the intensities of three nightglow emission features, which have different relationships to

*Supported by the National Science Foundation of China (40225011, 40336054), National Research Project (G2000078407), project of CAS (KZCX3-SW-217), International Collaboration Research Team Program of the Chinese Academy of Sciences and the China-Russia Joint Research Center on Space Weather, Chinese Academy of Sciences

Received 2005-06-10

(C)1994-2022 China Academic Journal Electronic Publishing House. All rights reserved. http://www.cnki.net

the atomic oxygen density and background density.

The OI (557.7 nm) airglow is strong emission line in the MLT region and relatively easy to be observed on the ground. Therefore plenty of ground-based experiments on OI (557.7 nm) airglow intensity had already been carried out in early research about airglow. Hitherto we have been observing OI (557.7 nm) airglow intensity for many years. Furthermore, some ground-based observation stations just observe OI (557.7 nm) airglow intensity, so it is impossible to obtain atomic oxygen density profile according to the ground-based method mentioned above. In order to solve this problem and take full advantage of long-term observation on OI (557.7 nm) airglow intensity to research the long-term variation trend of atomic oxygen density, we have to develop a new method by which the peak density of atomic oxygen can be estimated from OI (557.7 nm) airglow intensity.

The main objective of this paper is to discuss in theory the feasibility and the method of deducing the peak density of undisturbed atomic oxygen profile in the MLT region from the OI (557.7 nm) night airglow intensity. In Section 2, the theory of OI (557.7 nm) airglow emission is presented. In Section 3, we give the approximate expression for the atomic oxygen profile in the MLT region and take 120° E as an example to illuminate the method of determining the two parameters in the approximate expression and the method of deriving the peak density. In Section 4, the characteristics of inversion relative errors and their sources are discussed. The influence of variations in temperature on inversion errors is discussed in brief. At last, we give the inversion results of a set of atomic oxygen density profiles at the location 120° E, 45° N, on the hundredth midnight in a year. In Section 5 we present the summary.

2 The Photochemical Theory of OI (557.7 nm) Airglow Emission

The OI (557.7 nm) airglow is the production of the transition from $O(^1S)$ to $O(^1D)$. The photochemical reactions and the rate coefficients are listed in Table 1.

Table 1 Chemical reactions about the OI (557.7 nm) airglow

reaction	rate coefficient
$O(^3P) + O(^3P) + M \xrightarrow{\beta k_1} O_2^* + M$	$k_1 = 4.7 \times 10^{-33}(300/T)^2\ \mathrm{cm^6 \cdot s^{-1}}$
$O_2^* + O(^3P) \xrightarrow{\delta k_2^O} O(^1S) + O_2$	$\delta k_2^O = 6.0 \times 10^{-11}\ \mathrm{cm^3 \cdot s^{-1}}$
$O_2^* + O_2, N_2, O \xrightarrow{k_2^{O_2,N_2,O}} O_2, N_2, O$ (except $O(^1S)$)	
$O_2^* \xrightarrow{A_1} O_2 + h\nu$	$A_1 = 2.0 \times 10^{-2}\ \mathrm{s^{-1}}$
$O(^1S) + O_2 \xrightarrow{k_3} O + O_2$	$k_3 = 4.0 \times 10^{-12} \exp(-865/T)\mathrm{cm^3 \cdot s^{-1}}$
$O(^1S) \xrightarrow{A_2} O(^1D) + h\nu(557.7\ \mathrm{nm})$	$A_2 = 1.18\ \mathrm{s^{-1}}$
$O(^1S) \xrightarrow{A_3} O(^3P, ^1D) + h\nu(\mathrm{total})$	$A_3 = 1.35\ \mathrm{s^{-1}}$

Note: Units are $(\mathrm{s^{-1}})$, $(\mathrm{cm^{-3} \cdot s^{-1}})$, and $(\mathrm{cm^{-6} \cdot s^{-1}})$ for unimolecular, bimolecular, and termolecular reactions, respectively.

In Table 1, k_1 is the rate coefficient for three-body recombination of atomic oxygen. β_1 represents the fraction of recombination which occurs into the O_2^* state. k_2^o is the coefficient for quenching of O_2^* by $O(^3P)$. δ represents the fraction which occurs into the $O(^1S)$ state. $k_2^{O_2}$ and $k_2^{N_2}$ are the coefficients for quenching of O_2^* by O_2 and N_2 respectively. k_3 is the coefficient for quenching of $O(^1S)$ by O_2. A_1 and A_3 are the inversion O_2^* radiative lifetime and the inversion $O(^1S)$ radiative lifetime respectively. A_2 is the $O(^1S - {}^1D)$ transition probability, and T is the background atmosphere temperature.

When atomic oxygen density is in photochemistry equilibrium, the expression for OI (557.7 nm) airglow volume emission rate is given by

$$V_{\mathrm{OI(557.7\,nm)}} = A_2[O(^1S)] = \frac{A_2 k_1 [O]^3 [M]}{\{(A_3 + k_3[O_2])(C'^{(0)} + C'^{(1)}[O] + C'^{(2)}[O_2])\}}. \quad (1)$$

where $R = [N_2]/[O_2]$, $M = \{[O_2], [N_2]\}$,

(C)1994-2022 China Academic Journal Electronic Publishing House. All rights reserved. http://www.cnki.net

$C'^{(0)} = A_4/\beta\delta k_4^{O} \approx 0$, $C'^{(1)} = 1/\beta\delta = 211$,
$C'^{(2)} = (k_4^{O_2} + Rk_4^{N_2})/\beta\delta k_4^{O} = 15$.

It is apparent that $V_{OI(557.7\,nm)}$ approximately scale as $[O]^3[M]$. Therefore, $V_{OI(557.7\,nm)}$ is controlled by the atomic oxygen density. In addition, in the MLT region the atomic oxygen density increases sharply upwards from 80 km, maximizes around 98 km, and then decreases upwards. Therefore the OI (557.7 nm) airglow intensity is intensively affected by the peak density of atomic oxygen. And it is possible to deduce the peak density of atomic oxygen from the OI (557.7 nm) airglow intensity.

3 The Inversion Method

The inversion method introduced in this paper is based on the theory of the OI (557.7 nm) airglow emission described in Section 2 and the approximate expression for the vertical distribution of O.

3.1 The Approximation for O Profile

In Fig.1 the solid line represents the undisturbed atomic oxygen profile in the MLT region at the location 120° E, 45° N on the hundredth midnight in a year.

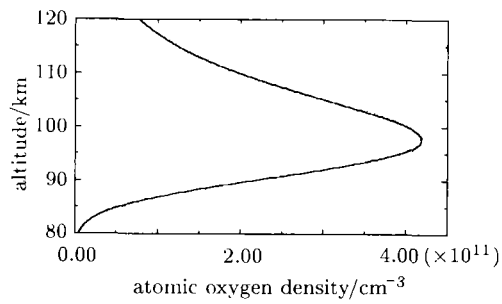


Fig.1 The atomic oxygen density profiles at 120° E, 45° N on the hundredth midnight in a year. Where the solid line is from the MSISE-90 model and the dashed line is the fitting result

Considering the vertical distribution features of the atomic oxygen density profiles in the MLT region, we can use the following expression approximate them:

$$[O]_z = [O]_{max} \exp\left[1 - \frac{Z - Z_{max}}{w} - \exp\frac{-(Z - Z_{max})}{w}\right]. \quad (2)$$

Where $[O]_{max}$ and Z_{max} are the atomic oxygen peak density and peak height, respectively. w is related to the shape of atomic oxygen density profile. Setting the $[O]_{max}$ in expression (2) to the peak density of the solid line profile and fitting the solid line profile using expression (2), we get the fitting result, the dashed line in Fig.1. The dashed line agrees with the solid line so well that we use expression (2) as the atomic oxygen distribution in the MLT region to do the inversion of the peak density of O.

3.2 The Inversion Method

In order to calculate the peak density of atomic oxygen using expression (2) and the OI (557.7 nm) airglow intensity, it is necessary to determine the values of Z_{max} and w in expression (2) beforehand.

We take 120° E as an example to study the method of determining the values of Z_{max} and w. Firstly we choose 32 undisturbed atomic oxygen density profiles from 90 km to 110 km, which are at 70° S, 50° S, 30° S, 10° S, 10°N, 30°N, 50° N and 70° N at midnight on the vernal equinox, the summer solstice, the autumnal equinox and the winter solstice respectively, from the MSISE-90 model, in which magnetic index Ap, daily $F_{10.7}$ flux for previous day, F_{107} and 3 month average of $F_{10.7}$ flux, F_{107A} are set to 4, 70, and 70, respectively. The profiles are then fitted by expression (2) using a nonlinear least squares fitting algorithm. In the fitting process, we make the value of $[O]_{max}$ in expression (2) equal to the peak density of the fitted profile. Then we obtain 32 sets of values of Z_{max} and w. Averaging them, respectively, we obtain the final result: $Z_{max} = 97.97504$, $w = 8.531177$. Consequently, expression (2) becomes following form:

$$[O] = [O]_{max} \exp\left[1 - \frac{Z - 97.97504}{8.531177} - \exp\frac{-(Z - 97.97504)}{8.531177}\right] \quad (3)$$

An integral of OI (557.7 nm) line volume emission rate from 80 km to 120 km can approximate the OI (557.7 nm) airglow intensity in the MLT region, because that the OI (557.7 nm) airglow layer is mainly situated between 80 km and 120 km in the MLT region. Therefore, (557.7 nm) airglow intensity can be represented by the following expression:

$$I_{OI(557.7\,nm)} = \int_{80}^{120} V_{OI(557.7\,nm)} dz$$

(C)1994-2022 China Academic Journal Electronic Publishing House. All rights reserved. http://www.cnki.net

$$= \int_{80}^{120} \frac{A_2 k_1 [\mathrm{O}]^3 [\mathrm{M}]}{\{(A_3 + k_3[\mathrm{O}_2])(C'^{(1)}[\mathrm{O}] + C'^{(2)}[\mathrm{O}_2])\}} \mathrm{d}z. \quad (4)$$

Here the vertical step is 0.1 km and the molecular oxygen density, molecular nitrogen density and temperature profiles are from the MSISE-90 model. The atomic oxygen density profile is from the MSISE-90 model in the process of calculating OI (557.7 nm) airglow intensity, which is used as the airglow observation. The expression (3) is used in the inversion of the peak density of O. The algorithm used in inversion process is direct inversion method.

4 The Inversion Results and the Errors Analysis

4.1 The Inversion Errors Analysis

We calculate the peak densities of the undisturbed atomic oxygen density profiles at the local time of 0000 for 0° E, 120° E and 120° W by using expression (3) and OI (557.7 nm) airglow intensities, respectively. The distributions of the inversion relative errors are shown in Fig.2.

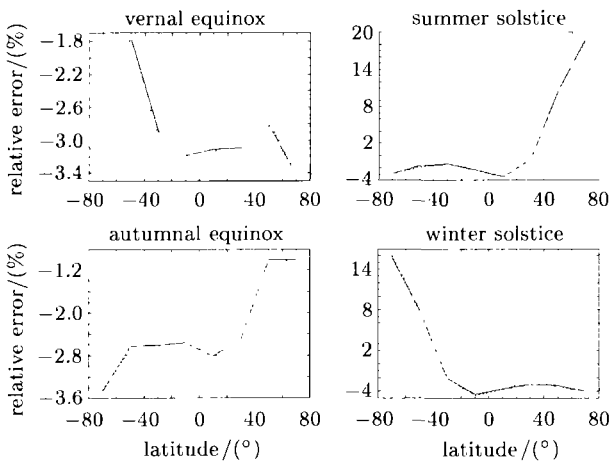


Fig.2 The distributions of the inversion relative error at 0° E (dashed lines), 120° E (solid lines) and 120° W (dotted lines) for four seasons

We can see three main features from Fig.2. Firstly, all errors are less than 5% except for those at high latitudes in the summer hemisphere, but which are less than 19%. So the expression (3) is valid at any longitude. Secondly, the distribution of the inversion errors in the Northern hemisphere is not symmetrical with that in the Southern hemisphere, and this is caused by the asymmetry of atomic oxygen distribution in the two hemispheres. Finally, the errors on the vernal equinox and the autumnal equinox and the errors at mid and low latitudes in the summer hemisphere are very small, but the errors at high latitudes in the summer hemisphere are large. This results from that the shapes of the atomic oxygen density profiles at high latitudes in the summer hemisphere markedly differ from those at other latitudes or in other seasons. Fig.3 gives four atomic oxygen density profiles at 120° E on the Summer Solstice and it can explain this.

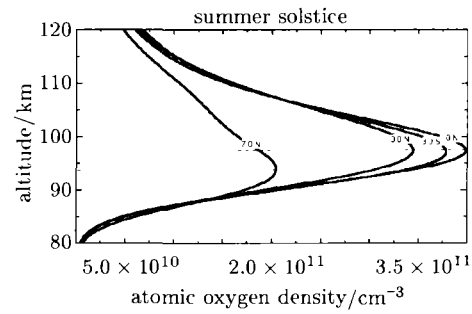


Fig.3 Atomic oxygen profiles at four latitudes at 120° E on the summer solstice in MSISE-90 model

We can see from Fig.3 that the peak height of atomic oxygen density varies with the latitude. The shapes of the atomic oxygen density profiles at mid and low latitudes are similar and their peak heights are around 98 km. However, the profile at 70° N is not as sharp as those at other latitudes. Its peak height is at about 94 km, which is 4 km lower than those at mid and low latitudes. So the value of $Z_{\max}$ for the profile at 70° N should be smaller than those for other latitudes and the value of w for the profile at 70° N should be larger than those for other latitudes when the profiles in Fig.3 are fitted by expression (2). Therefore when the profiles at high latitudes in the summer hemisphere are inversed by expression (3), the parameters of $Z_{\max}$ and w should be adjusted.

4.2 The Impact of Variations in Temperature on the Inversion Results

Because that k_1 and k_3 in expression (4) are the functions of temperature and the profiles of the [O], [N_2] and [O_2] are affected by temperature, the variations in temperature will impact on the inversion results. Fig.4 shows the distributions of inversion errors at 120° E when the background temperature decreases

(C)1994-2022 China Academic Journal Electronic Publishing House. All rights reserved. http://www.cnki.net

20 K and increases 20 K, respectively. And they are compared with the original distribution. Fig.4 indicates that the inversion errors are impacted by the variations in temperature but the influence is not significantly. So if there is error in the background temperature when we make inversion calculation, the peak density can also be estimated from OI (557.7 nm) airglow intensity through the method described above.

For a more detailed comparison we show the profiles of the inversion error distributions at different latitudes at 120° E when the variations in background temperature range from −50 K to +50 K in Fig.5. We see from Fig.5 that error for any latitude decreases with the increase in temperature.

4.3 An Example of the Inversion Results

The atomic oxygen density profiles at the location 120° E, 45° N at local time of 0:00 on the hundredth midnight in a year are inversed according to the method described above. The inversion errors are listed in Table 2. The original and the inversion profiles are shown in Fig.6.

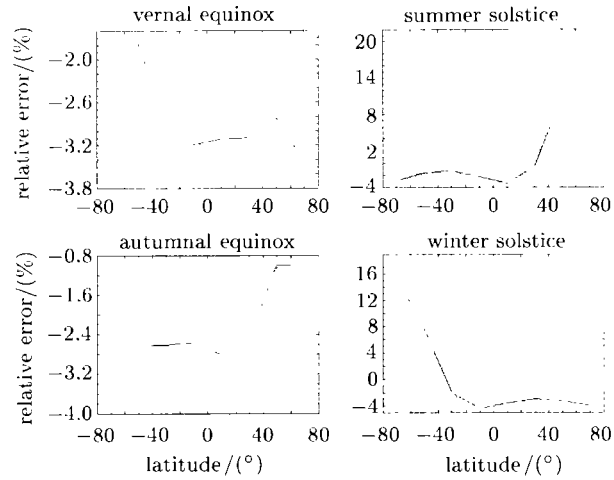


Fig.4 Comparison of error curves calculated from three background temperature profiles at 120° E. Where the dashed lines are for $T-20$ K, the solid lines are for T and the dotted lines are for $T+20$ K

Table 2 and Fig.6 indicate that the inversion peak densities and profiles around the peak heights agree very well with the true ones, respectively.

5 Summary

From above discussion we can get the following con-

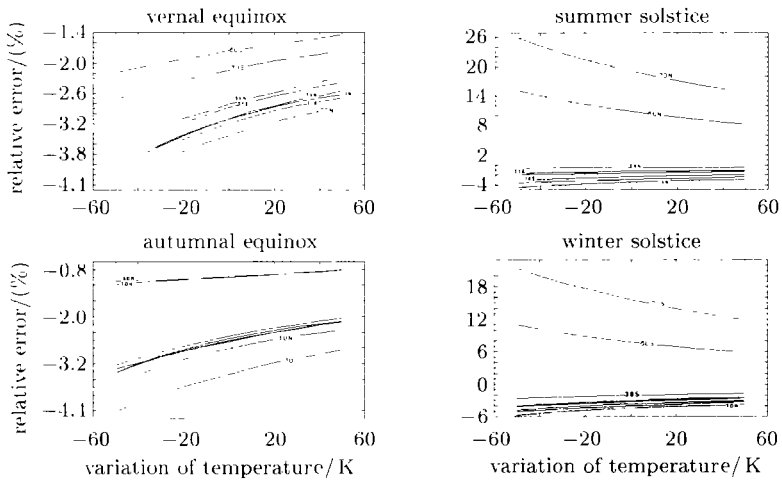


Fig.5 The relationship of the inversion errors with the variations in temperature at different latitudes at 120° E

Table 2 The inversion errors

background temperature/K	true peak density/cm^{-3}	inversion peak density/cm^{-3}	inversion relative error/(%)
$T-20$ K	$4.707\,60\times10^{11}$	$4.621\,10\times10^{11}$	−0.183 742
T	$4.189\,44\times10^{11}$	$4.119\,18\times10^{11}$	−0.167 716
$T+20$ K	$3.774\,10\times10^{11}$	$3.715\,92\times10^{11}$	−0.154 130

(C)1994-2022 China Academic Journal Electronic Publishing House. All rights reserved. http://www.cnki.net

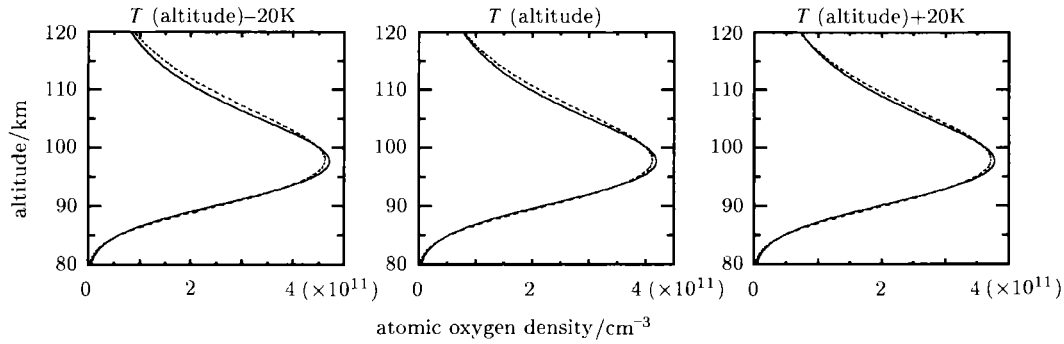


Fig.6 The inversed atomic oxygen density profiles (dashed lines) compared with the true profiles in MSISE-90 model (solid lines)

clusions. It is possible in theory to derive the peak density of undisturbed atomic oxygen profiles from the OI (557.7 nm) night airglow intensity in the MLT region. The values of $Z_{\max}$ and w in approximate expression (2) are determined through fitting the profiles at 120° E. Then the peak densities for different longitudes, latitudes and seasons are inversed by approximate expression (3) and OI (557.7 nm) night airglow intensities. The inversion results indicate that all inversion errors are less than 5% except for those at high latitudes in the summer hemisphere, which reaches 19%. This is caused by that the true values of $Z_{\max}$ and w at high latitudes in the summer hemisphere are markedly different from the values of $Z_{\max}$ and w in expression (3). In practical measurements, we can find more reliable values for $Z_{\max}$ and w at high latitudes in the summer hemisphere to decrease the inversion errors. Furthermore the influence of the variations in background temperature on the inversion errors is small and the inversion errors decrease with the increase in temperature.

Acknowledgement The authors wish to thank Liu Xiao *et al.* for useful discussion. This work was supported by the National Science Foundation of China (40225011, 40336054), National Research Project (G2000078407) and project of CAS (KZCX3-SW-217).

References

[1] Jiyao Xu, Yongfu Wu, Yongmei Wang, Liping Fu. Research on the criterion of gravity wave instability induced by photochemistry in polar mesopause region in summer. *Sci. China*, 2001, **31**:889—895 (in Chinese)

[2] Rodrigo R, López-Moreno J J, López-Gonzalez M J, García-Alvarez E. Atomic oxygen concentrations from OH and O_2 nightglow measurements. *Planet. Space Sci.*, 1989, **37**:49—60

[3] Lópezgonzález M J, Lópezmoreno J J, Rodrigo R. Atomic oxygen concentration from airglow measurements of atomic and molecular oxygen emissions in the nightglow. *Planet. Space. Sci.*, 1992, **40**:929—940

[4] Earlgood R. Determination of atomic oxygen density from rocket borne measurement of hydroxyl airglow. *Planet. Space Sci.*, 1976, **24**:389—395

[5] McDade I C, Lewellyn E J. Mesospheric oxygn atom densities inferred from night-tinme OH meinel band emission rates. *Planet. Space. Sci.*, 1988, **36**:897—905

[6] Russell J P, Lowe R P. Atomic oxygen profiles (80—94 km) derived from wind imaging interferometer/upper atmospheric research satellite measurements of the hydroxyl airglow: 1. Validation of technique. *J. Geophys. Res.*, 2003, **108** ACH 5-1, CiteID 4662, DOI 10.1029/2003JD003454

[7] Dandekar B S, Turtle J P. Atomic oxygen concentration from the measurement of the [OI] 5577Åemission of the airglow. *Planet, Space Sci.*, 1971, **19**:944—957

[8] David E Sisking *et al.* A comparison of measurements of the oxygen nightglow and atomic oxygen in the lower thermosphere. *Planet. Space Sci.*, 1991, **39**:627—639

[9] Gobbi D *et al.* Equatorial atomic oxygen profiles derived from rocket observations of OI 557.7 nm airglow emission. *Planet. Space Sci.*, 1992, **40**:775—781

[10] Stella M L Melo *et al.* Atomic oxygen concentrations from rocket airglow observations in the equatorial region. *J. Atmos. Terr. Phys.*, 1996, **58**:1935—1942

[11] Edith I. Reed and sushil chandra, the global characteristics of atmospheric emission in the lower thermosphere and their aeronomic implications. *J. Geophy. Res.*, 1975, **80**:3053—3062

[12] Rao M N M, Murty G S N. A new method of deducing the atomic oxygen density profiles in the lower thermosphere using ground-based night airglow observations. *J. Atmosp. Terr. Phys.*, 1981, **43**:1253—1264

[13] Haley C S, Mcdade I C, Melo S M L. An assessment of a method for recovering atomic oxygen density profiles from column integerated nightglow intensity measurements. *Adv. Space Res.*, 2001, **27**:1147—1152

[14] Stella M L Melo, IanC McDade, Hisao Takahashi. Atomic oxygen density profiles from ground-based nightglow measurements at 23°S. *J. Geophys. Res.*, **106**(D14):15 377—15 384

(C)1994-2022 China Academic Journal Electronic Publishing House. All rights reserved. http://www.cnki.net